Synergistic Effect of Elevated Device Temperature and Excess Charge Carriers on the Rapid Light-Induced Degradation of Perovskite Solar Cells

*Bo Chen, Jingfeng Song, Xuezeng Dai, Ye Liu, Peter N. Rudd, Xia Hong, and Jinsong Huang**

With power conversion efficiencies now reaching 24.2%, the major factor limiting efficient electricity generation using perovskite solar cells (PSCs) is their long-term stability. In particular, PSCs have demonstrated rapid degradation under illumination, the driving mechanism of which is yet to be understood. It is shown that elevated device temperature coupled with excess charge carriers due to constant illumination is the dominant force in the rapid degradation of encapsulated perovskite solar cells under illumination. Cooling the device to 20 °C and operating at the maximum power point improves the stability of $CH_3NH_3PbI_3$ solar cells over 100× compared to operation under open circuit conditions at 60 °C. Light-induced strain originating from photothermal-induced expansion is also observed in $CH_3NH_3PbI_3$, which excludes other light-induced-strain mechanisms. However, strain and electric field do not appear to play any role in the initial rapid degradation of $CH_3NH_3PbI_3$ solar cells under illumination. It is revealed that the formation of additional recombination centers in PSCs facilitated by elevated temperature and excess charge carriers ultimately results in rapid light-induced degradation. Guidance on the best methods for measuring the stability of PSCs is also given.

The power conversion efficiency (PCE) of organic–inorganic lead halide perovskite solar cells (PSCs) has continued to soar, reaching a certified value of 24.2% and surpassing most other thin film photovoltaic technologies.[1,2] Efforts in upscaling devices have yielded large area (>50 cm^2) perovskite modules with PCEs comparable to that of most commercial silicon modules.[3] This leaves the long-term stability of PSCs as the greatest challenge impeding their commercialization.[4] The dominant pathways for degradation of PSCs during exposure to light, moisture, oxygen, and elevated temperatures spawn from the instability of perovskite materials, charge transport layers, electrodes, as well as the interaction at the interfaces between them.[5–9] Many strategies have been reported to improve the stability of PSCs under operating conditions via composition engineering,[10–14] utilization of inorganic charge-transport layers,[15–18] and defect passivation.[19–22] Moisture causes reversible conversion of $CH_3NH_3PbI_3$ to a hydrated product,[23] and the trapped photoexcited charges can trigger the moisture-induced irreversible dissociation of perovskite materials into PbI_2, volatile CH_3NH_2, and HI.[23,24] When perovskite solar cells are exposed to light and oxygen, the reaction between generated superoxide (O_2^-) and perovskite materials results in rapid degradation.[25–27] The O_2^- species are created by the transfer of photoexcited electrons to molecular oxygen.[25–27] Thus, reducing the amount of trapped charges under illumination can improve the stability of PSCs under both moisture and oxygen.[23–27] Elevated temperature induces the degradation of PSCs through the decomposition of perovskites into PbI_2[7,28] or lead $(Pb)^0$/iodine $(I)^0$ defects,[29] as well as possible diffusion of the metal electrode into charge transport layers and perovskite films.[9,16,17,30] Among all these stresses, light-induced degradation seems to be most severe given that well-encapsulated silicon photovoltaic devices can last more than ten years, while most encapsulated PSCs last merely six months under realistic operating conditions.[4] Encapsulation can eliminate moisture- and oxygen-induced degradation but ultimately cannot avoid this intrinsic light-induced degradation.

Illumination of PSCs leads to a number of phenomena which all impacts perovskite solar cell stability, including: an increase in device temperature due to photothermal effect,[31,32] strain from photostriction[33–36] or thermal expansion,[37] photoexcited charge carriers,[38] and electric field due to built-in potential and photovoltage.[39] While several studies have reported perovskite solar cells with long-term stabilities exceeding 500 h, the

Dr. B. Chen, X. Dai, P. N. Rudd, Prof. J. Huang
Department of Applied Physical Sciences
University of North Carolina at Chapel Hill
Chapel Hill, NC 27599, USA
E-mail: jhuang@unc.edu
Dr. J. Song, Prof. X. Hong
Department of Physics and Astronomy & Nebraska Center for Materials and Nanoscience
University of Nebraska-Lincoln
Lincoln, NE 68588, USA
Y. Liu, Prof. J. Huang
Department of Mechanical and Materials Engineering
University of Nebraska-Lincoln
Lincoln, NB 68588, USA
The ORCID identification number(s) for the author(s) of this article can be found under https://doi.org/10.1002/adma.201902413.

DOI: 10.1002/adma.201902413

devices were measured at different operating temperatures, such as 85,[10,16] 60,[17] 45 °C,[40] and mostly room temperature.[41–45] In realistic operation conditions, the working temperatures of the solar panels are dependent on weather conditions and the environmental temperature of where they are installed, ranging from below –20 °C in cold arctic areas to over 80 °C in hot desert areas.[31,32] For the applications in tropical countries and even as building-integrated photovoltaics (BIPV) in temperate climates during summer, the solar cells can be heated by sunlight to 60–80 °C.[31,32] Therefore, it is important to know the impact of device operation temperature on the stability of PSCs during illumination. On the other hand, Zhao et al. first reported that the most perovskite films made by existing fabrication methods are strained due to the mismatched thermal expansion coefficients between perovskite films and substrates, and strain diminishes the long-term stability of PSCs.[46] Other studies confirmed the impact of strain on the stability of PSCs.[47–49] The lattice strain in perovskite film has been proposed to impact ion migration,[46] defect formation,[48] and carrier dynamics[50] in PSCs. Strain can be generated in perovskite films during device fabrication,[46,49,51] thermal expansion,[37,47,49] photostriction,[33–36] electrostriction,[52] or local lattice strain due to ionic size mismatch.[53] While strain-accelerated degradation of perovskite films is established,[46–49] whether the light-induced strain is the dominant driving force for degradation of perovskite solar cells still needs to be confirmed. Finally, the presence of excess photoexcited charge carriers has also been reported to accelerate ion migration in lead halide perovskite materials, hindering the stability of PSCs.[38,54,55] Given that these light-induced phenomena can all provide degradation pathways in PSCs under illumination, the dominant degradation mechanism(s) has yet to be identified.

In this study, we investigated the mechanism for the initial stage of light-induced degradation of encapsulated perovskite solar cells through analyzing the effects of light-induced heat, strain, electric field, and charge carriers. $CH_3NH_3PbI_3$ was chosen for this study, because it is the least stable perovskite composition. It is also a phase pure material allowing us to avoid the complexity of degradation related to phase segregation. We examined the impact of elevated operating temperature on the stability of encapsulated devices, and analyzed whether degradation originates from thermal expansion or the acceleration of other kinetic processes by high temperatures. We investigated the degradation rate of PSCs under excess charges at different device temperatures. The synergistic effect of elevated device temperature and excess charges on device degradation is discussed based on their impact on defect formation.

Our studies showed that the operating temperature of encapsulated $CH_3NH_3PbI_3$ solar cells plays an important role on the device stability. Under continuous 1 sun illumination at maximum power point (MPP), we observed that the working temperature of the device was elevated to around 60 °C and the PCE of the encapsulated device decayed rapidly within 6 h (**Figure 1**a). It should be noted that the stability of $CH_3NH_3PbI_3$ solar cells is significantly improved when the device is cooled to 20 °C by a thermoelectric cooler during illumination (Figure 1a), in agreement with previously reported work.[30] The impact of elevated temperature under illumination on device stability can be ascribed to thermal expansion, phase transition, or acceleration of kinetic processes, such as ion migration, defect formation, and chemical reactions at high temperature.

In order to understand the influence of photothermal-induced strain on device stability, we first need to characterize its magnitude compared to other sources of strain in $CH_3NH_3PbI_3$, such as photostriction and electrostriction. The light-induced strains of $CH_3NH_3PbI_3$ perovskite single crystals (Figure 1b) and thin films (Figure S1, Supporting Information) were measured by X-ray diffraction (XRD). In both cases, the detected XRD peak positions of $CH_3NH_3PbI_3$ continuously shifts to a smaller diffraction angle with increasing illumination time by a white LED with light intensity of 100 mW cm^{-2} (Figure 1b; Figure S1, Supporting Information). Meanwhile, the sample temperature was also gradually increased during illumination (Figure 1c). Figure 1d summarizes the change of strain and sample temperature of a (200) $CH_3NH_3PbI_3$ single crystal under illumination for 15 min, which reveals a linear relationship with a slope agreeing with the reported thermal expansion coefficient of $CH_3NH_3PbI_3$.[37] To further distinguish the contribution of strain from photostriction and thermal expansion, we turned the light on and off while either heating the sample to 53 °C (Figure 1e) or cooling the sample to 20 °C (Figure 1f). After the light was switched on or off, the temperature of the samples was then maintained for 10 min before measuring the diffraction pattern. We found that switching the light between on and off conditions has no influence on the position of XRD peaks for $CH_3NH_3PbI_3$, as long as the temperature remains constant. Moreover, the observed light-induced strain of $CH_3NH_3PbI_3$ perovskite here is orientation dependent (Figure S2, Supporting Information), while previously reported photostriction of $CH_3NH_3PbI_3$ is a uniform lattice expansion independent of crystalline orientation.[40,41] In addition to illuminating for several minutes, we also compared the thermal expansion and photostriction on a millisecond timescale in Figure S3b in the Supporting Information, and still found the thermal expansion to dominate the light-induced strain in $CH_3NH_3PbI_3$, with no photostriction detected within equipment sensitivity limitation. These results clearly show that light-induced strain is caused by thermal expansion, rather than photostriction in $CH_3NH_3PbI_3$. Besides photostriction, we also exclude the contributions of piezoelectricity and electrostriction to light-induced strain of $CH_3NH_3PbI_3$ in Figure S3c in the Supporting Information.

The elevated temperature could change strain in $CH_3NH_3PbI_3$, however, because the increase of temperature is automatically accompanied by thermal expansion, it is difficult to distinguish whether it is thermal expansion or the acceleration of kinetic processes playing a greater role in device photodegradation at elevated temperature. In order to find out the impact of strain, we introduced uniaxial strain into the perovskite films through bending a flexible $CH_3NH_3PbI_3$ solar cell made on flexible indium tin oxide (ITO)/polyethylene terephthalate (PET) substrates. Surprisingly, even under a large tensile strain of 0.3%, the bent device did not show any noticeable change in the PCE decay rate compared to the flat device during 3 h of illumination (Figure 1g). We recently found that the as-fabricated $CH_3NH_3PbI_3$ films bear large residual strain, due to the mismatched thermal expansions

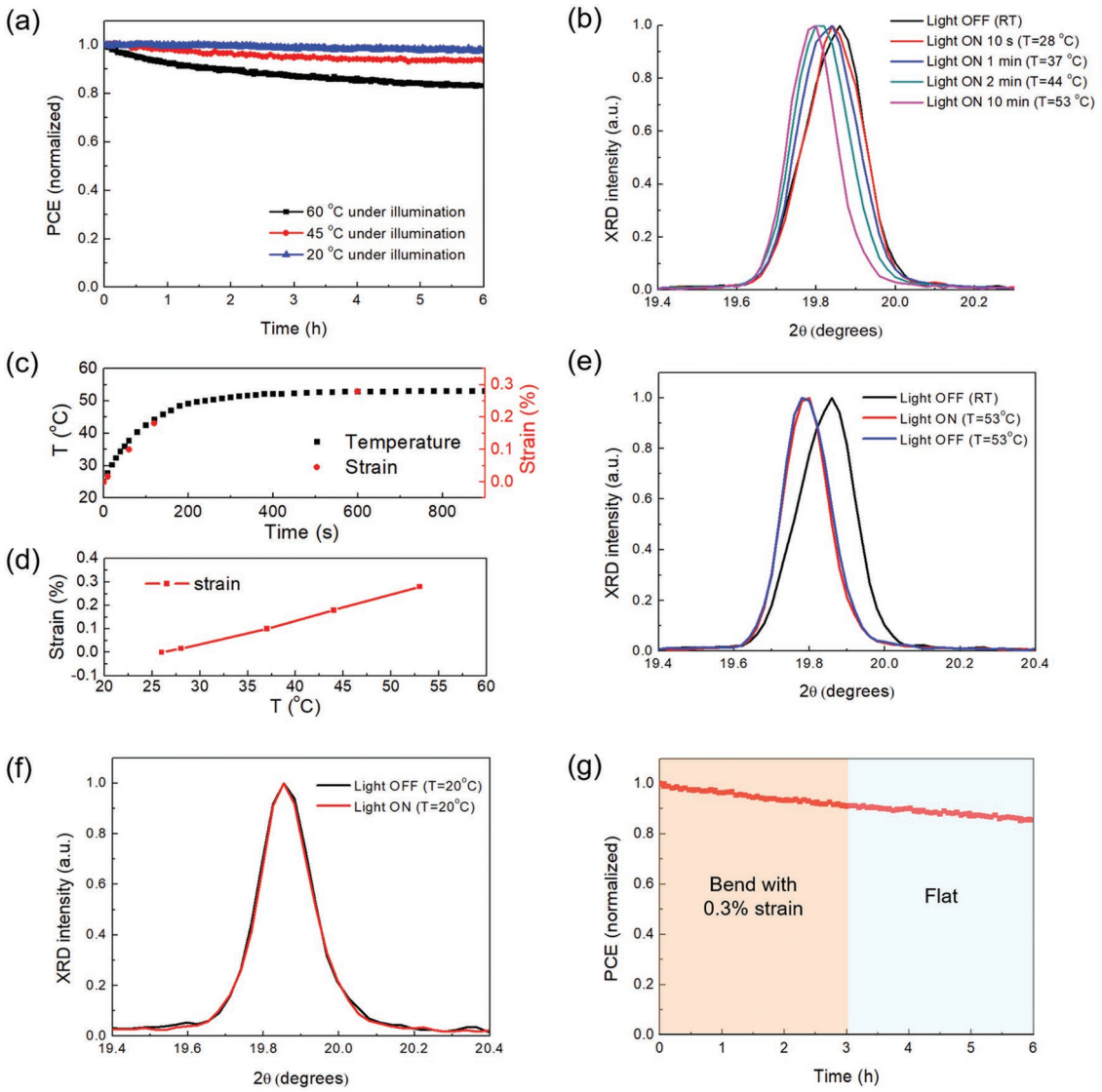

Figure 1. Impact of elevated device temperature and strain on stability of $CH_3NH_3PbI_3$ solar cell. a) PCE decay of encapsulated $CH_3NH_3PbI_3$ solar cells under 1 sun illumination at MPP condition with device temperature of 60, 45, and 20 °C. b) Shift in XRD peak of $CH_3NH_3PbI_3$ single crystal to smaller diffraction angle with increasing duration of illumination under 100 mW cm^{-2} white LED. c) Change of temperature and strain in $CH_3NH_3PbI_3$ single crystal with illumination duration time of 100 mW cm^{-2} white LED. d) Relation of light-induced strain and sample temperature for $CH_3NH_3PbI_3$ single crystal under illumination of 100 mW cm^{-2} white LED. e) XRD patterns of $CH_3NH_3PbI_3$ single crystal under light off at room temperature (RT), light (100 mW cm^{-2} white LED) on at 53 °C, and light off at 53 °C. f) XRD patterns of $CH_3NH_3PbI_3$ single crystal under light off at 20 °C and light on at 20 °C. g) PCE decay of unencapsulated flexible $CH_3NH_3PbI_3$ solar cells on ITO/PET substrate with and without bending under 1 sun illumination in N_2-filled gloveboxes.

between $CH_3NH_3PbI_3$ and the substrates.[46] Although heating the $CH_3NH_3PbI_3$ solar cells from 20 to 60 °C actually reduces this residual strain in $CH_3NH_3PbI_3$ films,[46] the device suffered accelerated degradation at elevated temperatures. This elucidates that the impact of elevated temperature on the initial rapid degradation in $CH_3NH_3PbI_3$ solar cells under illumination is dominated by heat rather than strain. As the reported residual strain influences the stability of perovskite film at a timescale of hundreds of hours under illumination,[46] it is not in conflict with the result of current study, because here we are exploring the dominant origin of light-induced degradation over 6 h.

We found that the phase transition of perovskite materials is not the dominant source of rapid light-induced degradation in PSCs. The degradation rates of $CH_3NH_3PbI_3$ solar cells at working temperatures of 45 and 60 °C, which is below and above tetragonal-to-cubic phase transition of $CH_3NH_3PbI_3$ (55 °C), respectively, are both accelerated compared to at 20 °C (Figure 1a). For other organic–inorganic halide perovskites without a phase transition at temperature range of 20–60 °C, such as $FA_{0.85}MA_{0.15}Pb(I_{0.85}Br_{0.15})_3$,[56–58] significant changes in degradation rates between 20 and 60 °C under illumination is still observed (Figure S4, Supporting Information).

The rapid degradation of $CH_3NH_3PbI_3$ solar cells under illumination is not solely due to elevated temperatures, but actually results from the combination of multiple light-induced factors. When the device temperature was maintained at 60 °C, the performance decayed faster when the illumination intensity was increased from 0.1 to 1 sun (**Figure 2**a). This indicates that besides temperature, the photoexcited charge carriers also play an important role on light-induced degradation of PSCs. Additional evidence for the impact of photoexcited charge carriers on the device degradation is that under open-circuit (OC) condition at 60 °C, the devices exhibited faster degradation than under short-circuit or MPP conditions at 60 °C (Figure 2b), likely due to a greater number of excess photoexcited carriers at open-circuit condition. Therefore, the impact of elevated temperature under illumination on the stability of PSCs is also modulated by the amount of excess charge carriers. This agrees with previous finding by Lin et al. that excess charge carriers challenge the stability of PSCs.[38] However, it is noted that cooling the device to 20 °C can also retard the degradation rate under open-circuit condition (Figure 2b), thus the low device working temperature can suppress the detrimental effects of excess charge carriers on device stability. Therefore, it is the synergistic effect of elevated device temperature and excess photoexcited charges that dominate the rapid light-induced degradation of PSCs.

We also considered the influence of photovoltage on the device stability under illumination. For a $CH_3NH_3PbI_3$ solar cell with V_{OC} of ≈1.1 V and thickness of 500 nm, the built-in electric field is calculated to be ≈2.2 V μm^{-1}. At MPP condition, the applied external bias of ≈0.9 V partially compensates the built-in potential, thus the net electric field across $CH_3NH_3PbI_3$ films is reduced to ≈ 0.4 V μm^{-1}. There is a large difference in the net electric field across $CH_3NH_3PbI_3$ films between the short-circuit condition and MPP condition; however, this large field difference did not result in a significant difference in PCE decay rate at both 60 and 20 °C (Figure 2b). Although the net electric field across the $CH_3NH_3PbI_3$ films is zero at open-circuit condition, the devices still showed faster degradation compared to short-circuit conditions (Figure 2b). Therefore, the electric field under the realistic operating conditions is not the dominant driving force for the light-induced degradation of PSCs. The varying degradation rates under different load conditions are then attributed to the change of excess charge carrier density.

Excess charge carriers can be introduced not only by illumination, but also by electrical injection. Figure 2c shows the change of photovoltaic performance of $CH_3NH_3PbI_3$ solar cells after charge injection under constant current density in dark condition. After electrical charge injection under a constant current density of 20 mA cm^{-2} at 60 °C in dark conditions for 2 h, where the applied bias was kept around 1.07 V, the PSCs exhibited significant degradation (Figure 2c). However, it should be noted that *J–V* curves remain unchanged if the injection current density reduces by two orders of magnitude to 0.2 mA cm^{-2}. This highlights the important role of excess carriers at 60 °C on the device stability. Additionally, charge injection at 20 °C with current density of 20 mA cm^{-2} (with bias around 1.17 V) in dark for 2 h did not result in obvious degradation of $CH_3NH_3PbI_3$ solar cells. This is not dominated by the change of electric field but results from the temperature difference during electrical charge injection, because the applied bias (1.07 V) for charge injection at 60 °C is smaller than the

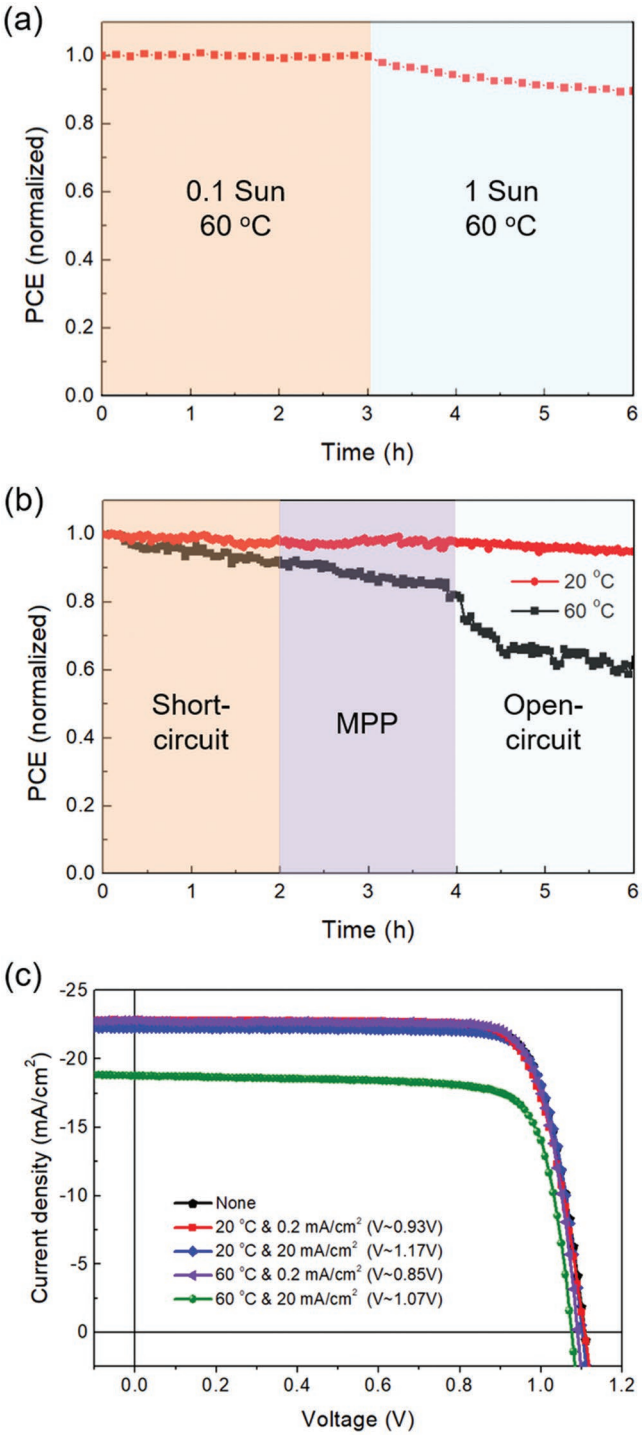

Figure 2. Impact of excess charges and temperature on stability of $CH_3NH_3PbI_3$ solar cell. a) PCE decay of encapsulated device under 0.1 and 1 sun illumination with device temperature maintained at 60 °C. b) PCE decay of encapsulated device at short-circuit, MPP, and open-circuit condition with device temperature of 60 and 20 °C, respectively. c) *J–V* curves of $CH_3NH_3PbI_3$ solar cell after charge injection under constant current density in dark for 2 h with different operating temperatures.

applied bias (1.17 V) for charge injection at 20 °C, but the PSCs degraded faster under the former condition. This result shows that the electrically injected excess charges coupled with the high device temperature can also impede PSC stability.

Considering that the heat and excess charge carriers are the dominant driving forces for rapid degradation of encapsulated perovskite solar cells under illumination, we anticipate that PSCs should demonstrate good long-term stability under illumination at MPP and low working temperature. $CH_3NH_3PbI_3$ solar cells have been reported to suffer from poor stability under illumination.[5] When operating the $CH_3NH_3PbI_3$ solar cells under open-circuit condition at 60 °C, its PCE rapidly reduced to 5% of the initial value after illumination under 1 sun for only 50 h. We found that for devices cooled to 20 °C during operation under MPP conditions, the PCE retained 92% of initial performance after illumination under 1 sun for 500 h (**Figure 3**). For comparison, the PCE of $CH_3NH_3PbI_3$ solar cells decreased to 92% of initial value after 40, 8, and 2 h of illumination under OC at 20 °C, MPP at 60 °C, and OC at 60 °C, respectively. At MPP conditions, cooling the device

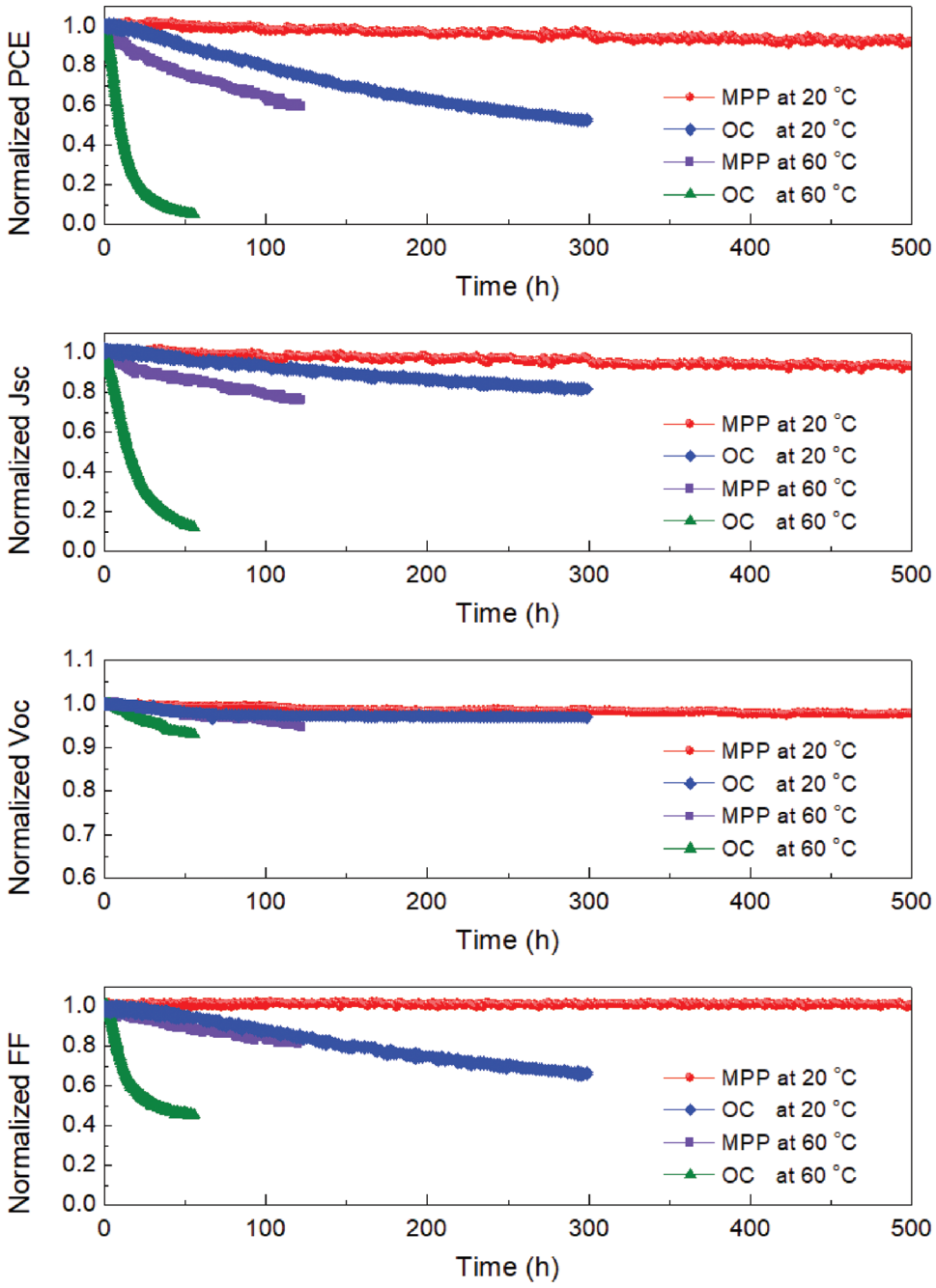

Figure 3. Long-term stability of encapsulated $CH_3NH_3PbI_3$ solar cells under 1 sun illumination under MPP at 20 °C, OC (open circuit) at 20 °C, MPP at 60 °C, and OC at 60 °C, respectively.

working temperature from 60 to 20 °C increased the device lifetime by over 50 times. Under open circuit conditions, even though the PSCs exhibited fast light-induced degradation at 60 °C, cooling the device to 20 °C also significantly improved the device stability. Therefore, it is the combined stress from elevated device temperature and increased excess charge carrier density that lead to the rapid degradation of $CH_3NH_3PbI_3$ solar cells under illumination. We found that the accelerated degradation of PSCs at elevated temperatures and more excess charge carriers under illumination is a general phenomenon in other halide perovskites PSCs. A similar degradation behavior was observed for perovskite solar cells with compositions which are frequently reported for improved performance, as shown in Figure S4 in the Supporting Information.

The degradation of $CH_3NH_3PbI_3$ solar cells under illumination can originate from the formation of additional recombination centers during operation. In **Figure 4**, we monitored the change of trap density of states (tDOS) and carrier recombination lifetimes in the device after light soaking under various conditions. After illumination under MPP and OC conditions at both 20 and 60 °C for 2 h, we found that the resulting photovoltaic performance is significantly reduced only under OC condition at 60 °C (Figure 3). We characterized the change of tDOS at different trap depths by thermal admittance spectroscopy in Figure 4a. After illumination under open circuit condition at 60 °C for 2 h, the tDOS in the deeper trap region (0.37–0.5 eV) is increased, and these deeper energies are assigned to defects at the film interface.[21,59] The tDOS remained almost constant after 2 h of illumination under MPP at 20 °C, under open circuit at 20 °C, or under MPP at 60 °C. The transient photovoltage (TPV) measurements show that the carrier recombination lifetime and V_{OC} of $CH_3NH_3PbI_3$ solar cells were decreased after illuminating under OC condition at 60 °C for 2 h (Figure 4b), with little change for the other three cases. Therefore, it is the formation of additional nonradiative recombination centers at perovskite films during illumination that drives the device degradation process. It is thus evident that low device working temperatures or operation under MPP condition can suppress the generation of nonradiative recombination centers under illumination and slow the degradation rate.

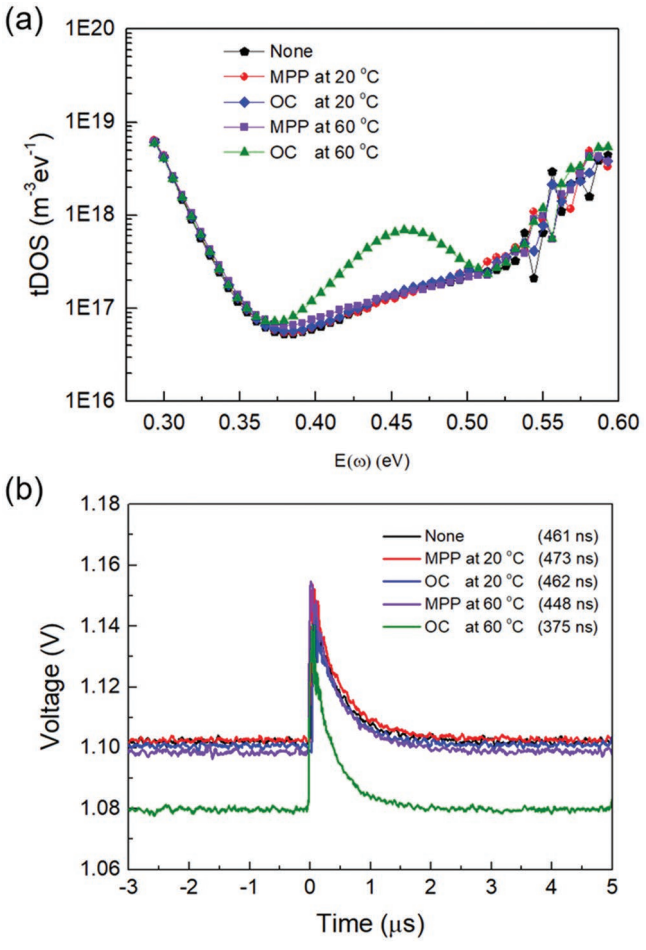

Figure 4. Defect formation during degradation of PSCs under illumination. Evolution of device a) tDOS and b) TPV for $CH_3NH_3PbI_3$ solar cells after illumination under MPP at 20 °C, OC at 20 °C, MPP at 60 °C, and OC at 60 °C for 2 h, respectively.

It is seen that all photovoltaic parameters, V_{OC}, J_{SC}, FF, and PCE, of PSCs deteriorate after illumination, as shown in Figure 3 and Figure S5 in the Supporting Information. The formation of additional nonradiative recombination centers after illumination reduces the carrier lifetime, thus decreasing the J_{SC}, V_{OC}, and FF of PSCs. Defect formation under illumination is described as a thermodynamic process. Low device working temperature can slow down the defect formation process and thus reduce the degradation rate of PSCs under illumination. Defect density reaches equilibrium due to a thermodynamic balance between the processes of defect annihilation and defect generation, and the excess charge carriers are speculated to push the equilibrium to more defect generation. Some mechanisms about the impact of excess photoexcited charges on the defect generation in perovskite films has been reported previously.[38,54,55] Our previous study has shown that the photoexcited excess charges could reduce the ion migration activation energy in lead halide perovskite materials by neutralizing the charged vacancies and thus reducing dragging force associated with ion migration.[38] The accelerated ion migration may facilitate the defect generation, because the migration of ions or vacancies from surface or grain boundaries into perovskite grains or charge transport layers can cause additional defects. Several other mechanisms are also reported for the generation of more defects under higher excess carrier concentration, such as stabilization of the iodide Frenkel defects by excess photoexcited electrons,[54] and neutralization of charged iodide ions by photoexcited holes.[55] The detailed mechanism for what types of defects impact the light-induced degradation of PSCs requires additional studies. Different strategies to avoid the defect formation, such as defect passivation, composition engineering, and efficient charge extraction, can improve the long-term stability of PSCs under illumination.

In summary, we investigated the mechanism of light-induced degradation of encapsulated perovskite solar cells by analyzing the impact of different light-induced factors, including heat, strain, excess charge carriers, and photovoltage. Our study showed that the elevated device temperature together with excess charges is the dominant source for the rapid degradation of perovskite solar cells under illumination. The thermal

expansion due to elevated device temperature under illumination dominates the light-induced strain in $CH_3NH_3PbI_3$ perovskite, while no photostriction is observed in $CH_3NH_3PbI_3$. However, strain plays a minor role on the rapid initial degradation of PSCs under illumination compared to the coupling effect of high temperature and excess charge carriers. The high device temperature and excess charge carriers facilitate the thermodynamic process of defect formation and can accelerate device degradation under illumination. Operation of PSCs under maximum power point at low temperature condition can thus improve the device's long-term stability. Considering that the realistic operation temperature of PSCs under sunlight at some outdoor conditions can reach 60–80 °C, it is important to achieve long-term stability of PSCs at elevated working temperature for their future commercialization.

Experimental Section

Perovskite Sample Fabrication: XRD sample of $CH_3NH_3PbI_3$ single crystals were grown on poly(triaryl amine) (PTAA)-coated ITO/glass through hydrophobic interface confined method, and more details are described in the previous studies.[52] The thickness of $CH_3NH_3PbI_3$ single crystal was 40 µm. $CH_3NH_3PbI_3$ single crystal powder was prepared by milling the millimeter size $CH_3NH_3PbI_3$ single crystal into ground powder. XRD sample of 500 nm $CH_3NH_3PbI_3$ thin film on PTAA-coated ITO/glass was prepared by N_2 gas blow assisted doctoral blading of 1.3 M $CH_3NH_3PbI_3$ precursor in 2-methoxyethanol with 2 vol% dimethyl sulfoxide, 0.1 wt% MA_2HPO_2, and 0.05 wt% L-α-phosphatidylcholine, and followed with annealing at 70 °C for 10 min and 100 °C for 25 min. For the $CH_3NH_3PbI_3$ perovskite solar cells, the bladed $CH_3NH_3PbI_3$ thin films on PTAA-coated ITO/glasses were then coated with consecutively thermally evaporated layers of 25 nm C_{60}, 6 nm BCP, and 90 nm Cu. For the other perovskite solar cells in Figure S4 in the Supporting Information, 1.4 M corresponding perovskite precursor (with mixed solvent of DMF:DMSO = 4:1 vol ratio) was spun onto the PTAA-coated ITO/glasses at 4000 rpm for 30 s, and the sample was quickly washed with 130 µL of toluene at the 25th s of spin-coating process; subsequently, the sample was annealed at 65 °C for 10 min and 100 °C (FAMA and CsFAMA) or 120 °C (for CsFA) for 15 min; followed by the consecutive thermal evaporation of 25 nm C_{60}, 6 nm BCP, and 90 nm Cu. The perovskite solar cells on ITO/glass substrate were encapsulated by Gorilla clear epoxy with a glass slide as a barrier layer. The flexible $CH_3NH_3PbI_3$ solar cells were prepared by bladed $CH_3NH_3PbI_3$ thin films on ITO/PET substrate followed with annealing and thermally evaporating of C_{60}, BCP, and Cu.

Measuring Light-Induced Strain by XRD: The XRD patterns were characterized by Bruker-AXS D8 Discover diffractometer with Vantec-500 area detector and Cu K-alpha radiation (wavelength 1.54 Å). The beam size of X-ray was 1 mm. The sample temperature during XRD measurement was controlled by the XRD sample stage with cooling and heating function. During the XRD measurement, white LED with a light intensity of 100 mW cm^{-2} was illuminated on the samples when light was needed. The sample temperature was monitored by the in situ thermometer in the XRD sample stage.

Device Photostability Measurement: Current–voltage measurements were recorded using a Keithley 2400 Source-Measure Unit under simulated AM 1.5G irradiation (100 mW cm^{-2}) by a plasma lamp in ambient air without any ultraviolet filter. The device efficiency was calculated based on current–voltage measurement. The devices were illuminated under continuous 100 mW cm^{-2} irradiation by plasma lamp. For cooling condition, the devices were mounted on a temperature control stage to maintain the device temperature at 20 °C. For the flexible $CH_3NH_3PbI_3$ solar cells on ITO/PET substrate, the current–voltage measurements were carried out at bending condition and at flat condition without encapsulation each for 3 h in N_2-filled gloveboxes. During the light soaking of encapsulated $CH_3NH_3PbI_3$ solar cells on ITO/glass substrate, the devices were operated under different electrical loads: short-circuit, open-circuit, or connected to a resistor so that it worked at its maximum power point.

Device Characterization: The transient photovoltage was measured under AM 1.5G illumination with pulse of 337 nm laser (SRS NL 100 Nitrogen Laser, pulse width was less than 3.5 ns) by digital oscilloscope (DOS-X 3104A). The input impedance of the oscilloscope was set to 1 MΩ. The ΔV caused by the laser pulse was controlled to be less than 5% of the V_{OC} under AM 1.5G illumination. Thermal admittance spectroscopy was measured by an E4980A Precision LCR Meter from Agilent at frequencies between 0.02 and 2000 kHz, with more details in the previous study.[59]

Supporting Information

Supporting Information is available from the Wiley Online Library or from the author.

Acknowledgements

The information, data, or work presented herein was also funded by the Office of Naval Research under award N00014-17-1-2727 and the National Science Foundation (NSF) under award No. DMR-1420645.

Conflict of Interest

The authors declare no conflict of interest.

Keywords

energy generation, light-induced degradation, perovskite solar cells

Received: April 15, 2019
Revised: June 3, 2019
Published online: July 4, 2019

[1] Q. Jiang, Y. Zhao, X. Zhang, X. Yang, Y. Chen, Z. Chu, Q. Ye, X. Li, Z. Yin, J. You, *Nat. Photonics* **2019**, *13*, 460.
[2] Cell efficiency chart, https://www.nrel.gov/pv/cell-efficiency.html (accessed: April 2019).
[3] Y. Deng, X. Zheng, Y. Bai, Q. Wang, J. Zhao, J. Huang, *Nat. Energy* **2018**, *3*, 560.
[4] N.-G. Park, M. Grätzel, T. Miyasaka, K. Zhu, K. Emery, *Nat. Energy* **2016**, *1*, 16152.
[5] D. Bryant, N. Aristidou, S. Pont, I. Sanchez-Molina, T. Chotchunang atchaval, S. Wheeler, J. R. Durrant, S. A. Haque, *Energy Environ. Sci.* **2016**, *9*, 1655.
[6] Q. Wang, B. Chen, Y. Liu, Y. Deng, Y. Bai, Q. Dong, J. Huang, *Energy Environ. Sci.* **2017**, *10*, 516.
[7] G. Divitini, S. Cacovich, F. Matteocci, L. Cina, A. Di Carlo, C. Ducati, *Nat. Energy* **2016**, *1*, 15012.
[8] A. Guerrero, J. You, C. Aranda, Y. S. Kang, G. Garcia-Belmonte, H. Zhou, J. Bisquert, Y. Yang, *ACS Nano* **2016**, *10*, 218.
[9] K. Domanski, J.-P. Correa-Baena, N. Mine, M. K. Nazeeruddin, A. Abate, M. Saliba, W. Tress, A. Hagfeldt, M. Grätzel, *ACS Nano* **2016**, *10*, 6306.
[10] M. Saliba, T. Matsui, K. Domanski, J. Y. Seo, A. Ummadisingu, S. M. Zakeeruddin, J. P. Correa-Baena, W. R. Tress, A. Abate, A. Hagfeldt, M. Gratzel, *Science* **2016**, *354*, 206.

[11] D. P. McMeekin, G. Sadoughi, W. Rehman, G. E. Eperon, M. Saliba, M. T. Hoerantner, A. Haghighirad, N. Sakai, L. Korte, B. Rech, M. B. Johnston, L. M. Herz, H. J. Snaith, *Science* **2016**, *351*, 151.

[12] M. Saliba, T. Matsui, J. Y. Seo, K. Domanski, J. P. Correa-Baena, M. K. Nazeeruddin, S. M. Zakeeruddin, W. Tress, A. Abate, A. Hagfeldt, M. Gratzel, *Energy Environ. Sci.* **2016**, *9*, 1989.

[13] Z. P. Wang, Q. Q. Lin, F. P. Chmiel, N. Sakai, L. M. Herz, H. J. Snaith, *Nat. Energy* **2017**, *2*, 17135.

[14] G. Grancini, C. Roldan-Carmona, I. Zimmermann, E. Mosconi, X. Lee, D. Martineau, S. Narbey, F. Oswald, F. De Angelis, M. Graetzel, M. K. Nazeeruddin, *Nat. Commun.* **2017**, *8*, 15684.

[15] Q. Jiang, L. Q. Zhang, H. L. Wang, X. L. Yang, J. H. Meng, H. Liu, Z. G. Yin, J. L. Wu, X. W. Zhang, J. B. You, *Nat. Energy* **2017**, *2*, 16177.

[16] S. Seo, S. Jeong, C. Bae, N. G. Park, H. Shin, *Adv. Mater.* **2018**, *30*, 1801010.

[17] N. Arora, M. I. Dar, A. Hinderhofer, N. Pellet, F. Schreiber, S. M. Zakeeruddin, M. Grätzel, *Science* **2017**, *358*, 768.

[18] J. B. You, L. Meng, T. B. Song, T. F. Guo, Y. Yang, W. H. Chang, Z. R. Hong, H. J. Chen, H. P. Zhou, Q. Chen, Y. S. Liu, N. De Marco, Y. Yang, *Nat. Nanotechnol.* **2016**, *11*, 75.

[19] X. Li, M. I. Dar, C. Y. Yi, J. S. Luo, M. Tschumi, S. M. Zakeeruddin, M. K. Nazeeruddin, H. W. Han, M. Grätzel, *Nat. Chem.* **2015**, *7*, 703.

[20] L. Liu, S. Huang, Y. Lu, P. F. Liu, Y. Z. Zhao, C. B. Shi, S. Y. Zhang, J. F. Wu, H. Z. Zhong, M. L. Sui, H. P. Zhou, H. B. Jin, Y. J. Li, Q. Chen, *Adv. Mater.* **2018**, *30*, 1800544.

[21] X. P. Zheng, B. Chen, J. Dai, Y. J. Fang, Y. Bai, Y. Z. Lin, H. T. Wei, X. C. Zeng, J. S. Huang, *Nat. Energy* **2017**, *2*, 17102.

[22] D. Q. Bi, P. Gao, R. Scopelliti, E. Oveisi, J. S. Luo, M. Grätzel, A. Hagfeldt, M. K. Nazeeruddin, *Adv. Mater.* **2016**, *28*, 2910.

[23] A. M. A. Leguy, Y. Hu, M. Campoy-Quiles, M. I. Alonso, O. J. Weber, P. Azarhoosh, M. van Schilfgaarde, M. T. Weller, T. Bein, J. Nelson, P. Docampo, P. R. F. Barnes, *Chem. Mater.* **2015**, *27*, 3397.

[24] N. Ahn, K. Kwak, M. S. Jang, H. Yoon, B. Y. Lee, J.-K. Lee, P. V. Pikhitsa, J. Byun, M. Choi, *Nat. Commun.* **2016**, *7*, 13422.

[25] N. Aristidou, C. Eames, I. Sanchez-Molina, X. Bu, J. Kosco, M. S. Islam, S. A. Haque, *Nat. Commun.* **2017**, *8*, 15218.

[26] N. Aristidou, I. Sanchez-Molina, T. Chotchuangchutchaval, M. Brown, L. Martinez, T. Rath, S. A. Haque, *Angew. Chem.* **2015**, *127*, 8326.

[27] A. J. Pearson, G. E. Eperon, P. E. Hopkinson, S. N. Habisreutinger, J. T. W. Wang, H. J. Snaith, N. C. Greenham, *Adv. Energy Mater.* **2016**, *6*, 1600014.

[28] T. Matsui, T. Yamamoto, T. Nishihara, R. Morisawa, T. Yokoyama, T. Sekiguchi, T. Negami, *Adv. Mater.* **2019**, *31*, 1806823.

[29] L. G. Wang, H. P. Zhou, J. N. Hu, B. L. Huang, M. Z. Sun, B. W. Dong, G. H. J. Zheng, Y. Huang, Y. H. Chen, L. Li, Z. Q. Xu, N. X. Li, Z. Liu, Q. Chen, L. D. Sun, C. H. Yan, *Science* **2019**, *363*, 265.

[30] K. Domanski, E. A. Alharbi, A. Hagfeldt, M. Grätzel, W. Tress, *Nat. Energy* **2018**, *3*, 61.

[31] A. McEvoy, T. Markvart, L. Castaner, *Practical Handbook of Photovoltaics: Fundamentals and Applications*, Elsevier, Amsterdam **2012**.

[32] S. A. Kalogirou, *Solar Energy Engineering: Processes and Systems*, Academic Press, San Diego, CA **2014**.

[33] Y. Zhou, L. You, S. Wang, Z. Ku, H. Fan, D. Schmidt, A. Rusydi, L. Chang, L. Wang, P. Ren, L. Chen, G. Yuan, L. Chen, J. Wang, *Nat. Commun.* **2016**, *7*, 11193.

[34] H. Tsai, R. Asadpour, J.-C. Blancon, C. C. Stoumpos, O. Durand, J. W. Strzalka, B. Chen, R. Verduzco, P. M. Ajayan, S. Tretiak, J. Even, M. A. Alam, M. G. Kanatzidis, W. Y. Nie, A. D. Mohite, *Science* **2018**, *360*, 67.

[35] T. C. Wei, H. P. Wang, T. Y. Li, C. H. Lin, Y. H. Hsieh, Y. H. Chu, J. H. He, *Adv. Mater.* **2017**, *29*, 1701789.

[36] X. Wu, L. Z. Tan, X. Shen, T. Hu, K. Miyata, M. T. Trinh, R. Li, R. Coffee, S. Liu, D. A. Egger, I. Makasyuk, Q. Zheng, A. Fry, J. S. Robinson, M. D. Smith, B. Guzelturk, H. I. Karunadasa, X. Wang, X. Zhu, L. Kronik, A. M. Rappe, A. M. Lindenberg, *Sci. Adv.* **2017**, *3*, e1602388.

[37] T. J. Jacobsson, L. J. Schwan, M. Ottosson, A. Hagfeldt, T. Edvinsson, *Inorg. Chem.* **2015**, *54*, 10678.

[38] Y. Lin, B. Chen, Y. Fang, J. Zhao, C. Bao, Z. Yu, Y. Deng, P. N. Rudd, Y. Yan, Y. Yuan, J. Huang, *Nat. Commun.* **2018**, *9*, 4981.

[39] J. M. Azpiroz, E. Mosconi, J. Bisquert, F. De Angelis, *Energy Environ. Sci.* **2015**, *8*, 2118.

[40] S. Wu, R. Chen, S. Zhang, B. H. Babu, Y. Yue, H. Zhu, Z. Yang, C. Chen, W. Chen, Y. Huang, S. F. Fang, T. Liu, L. Han, W. Chen, *Nat. Commun.* **2019**, *10*, 1161.

[41] H. R. Tan, A. Jain, O. Voznyy, X. Z. Lan, F. P. G. de Arquer, J. Z. Fan, R. Quintero-Bermudez, M. J. Yuan, B. Zhang, Y. C. Zhao, F. J. Fan, P. C. Li, L. N. Quan, Y. B. Zhao, Z. H. Lu, Z. Y. Yang, S. Hoogland, E. H. Sargent, *Science* **2017**, *355*, 722.

[42] J. A. Christians, P. Schulz, J. S. Tinkham, T. H. Schloemer, S. P. Harvey, B. J. T. de Villers, A. Sellinger, J. J. Berry, J. M. Luther, *Nat. Energy* **2018**, *3*, 68.

[43] S. H. Turren-Cruz, A. Hagfeldt, M. Saliba, *Science* **2018**, *362*, 449.

[44] S. S. Shin, E. J. Yeom, W. S. Yang, S. Hur, M. G. Kim, J. Im, J. Seo, J. H. Noh, S. I. Seok, *Science* **2017**, *356*, 167.

[45] Y. Hou, X. Y. Du, S. Scheiner, D. P. McMeekin, Z. P. Wang, N. Li, M. S. Killian, H. W. Chen, M. Richter, I. Levchuk, N. Schrenker, E. Spiecker, T. Stubhan, N. A. Luechinger, A. Hirsch, P. Schmuki, H. P. Steinruck, R. H. Fink, M. Halik, H. J. Snaith, C. J. Brabec, *Science* **2017**, *358*, 1192.

[46] J. Zhao, Y. Deng, H. Wei, X. Zheng, Z. Yu, Y. Shao, J. E. Shield, J. Huang, *Sci. Adv.* **2017**, *3*, eaao5616.

[47] C. Ramirez, S. K. Yadavalli, H. F. Garces, Y. Y. Zhou, N. P. Padture, *Scr. Mater.* **2018**, *150*, 36.

[48] T. W. Jones, A. Osherov, M. Alsari, M. Sponseller, B. C. Duck, Y. K. Jung, C. Settens, F. Niroui, R. Brenes, C. V. Stan, Y. Li, M. Abdi-Jalebi, N. Tamura, J. E. Macdonald, M. Burghammer, R. H. Friend, V. Bulovic, A. Walsh, G. J. Wilson, S. Lilliu, S. D. Stranks, *Energy Environ. Sci.* **2019**, *12*, 596.

[49] N. Rolston, K. A. Bush, A. D. Printz, A. Gold-Parker, Y. C. Ding, M. F. Toney, M. D. McGehee, R. H. Dauskardt, *Adv. Energy Mater.* **2018**, *8*, 1802139.

[50] C. Zhu, X. X. Niu, Y. H. Fu, N. X. Li, C. Hu, Y. H. Chen, X. He, G. R. Na, P. F. Liu, H. C. Zai, Y. Ge, Y. Lu, X. X. Ke, Y. Bai, S. H. Yang, P. W. Chen, Y. J. Li, M. L. Sui, L. J. Zhang, H. P. Zhou, Q. Chen, *Nat. Commun.* **2019**, *10*, 815.

[51] K. A. Bush, N. Rolston, A. Gold-Parker, S. Manzoor, J. Hausele, Z. J. Yu, J. A. Raiford, R. Cheacharoen, Z. C. Holman, M. F. Toney, *ACS Energy Lett.* **2018**, *3*, 1225.

[52] B. Chen, T. Li, Q. Dong, E. Mosconi, J. Song, Z. Chen, Y. Deng, Y. Liu, S. Ducharme, A. Gruverman, F. De Angelis, J. Huang, *Nat. Mater.* **2018**, *17*, 1020.

[53] M. I. Saidaminov, J. Kim, A. Jain, R. Quintero-Bermudez, H. R. Tan, G. K. Long, F. R. Tan, A. Johnston, Y. C. Zhao, O. Voznyy, E. H. Sargent, *Nat. Energy* **2018**, *3*, 648.

[54] D.-Y. Son, S.-G. Kim, J.-Y. Seo, S.-H. Lee, H. Shin, D. Lee, N.-G. Park, *J. Am. Chem. Soc.* **2018**, *140*, 1358.

[55] G. Y. Kim, A. Senocrate, T.-Y. Yang, G. Gregori, M. Grätzel, J. Maier, *Nat. Mater.* **2018**, *17*, 445.

[56] L. K. Ono, E. J. Juarez-Perez, Y. B. Qi, *ACS Appl. Mater. Interfaces* **2017**, *9*, 30197.

[57] W. S. Yang, J. H. Noh, N. J. Jeon, Y. C. Kim, S. Ryu, J. Seo, S. I. Seok, *Science* **2015**, *348*, 1234.

[58] T. Leijtens, K. Bush, R. Cheacharoen, R. Beal, A. Bowring, M. D. McGehee, *J. Mater. Chem. A* **2017**, *5*, 11483.

[59] Y. Shao, Z. Xiao, C. Bi, Y. Yuan, J. Huang, *Nat. Commun.* **2014**, *5*, 5784.